Article scientifique   Article   2017

Accepted version   Open Access

Detecting Perfusion Pattern based on the Background Low-frequency Fluctuation in Resting-State Functional MRI Data and its Influence on Resting-State Networks: An Iterative Post-processing Approach

Qian, Tianyi; Zanchi, Davide; Rodriguez, Cristelle; Ackermann, Marine; Giannakopoulos, Panteleimon; Haller, Sven

1

COVER PAGE

Title

Detecting Perfusion Pattern based on the Background Low-frequency Fluctuation in Resting-State Functional MRI Data and its Influence on resting state networks: an Iterative post-processing approach.

Authors

Tianyi Qian[1]*, Davide Zanchi[2]*, Cristelle Rodriguez[3], Marine Ackermann[3], Panteleimon Giannakopoulos[3,4], Sven Haller[4,5,6,7]

*Co-first authors.

Affiliations

1 MR Collaboration, Siemens Healthcare China, Beijing, China

2 Department of Psychiatry (UPK), University of Basel, Basel, Switzerland

3 Department of Mental Health and Psychiatry, University Hospitals of Geneva, Switzerland

4 Faculty of Medicine of the University of Geneva, Switzerland

5 Affidea Carouge Radiologic Diagnostic Center, Geneva, Switzerland

6 Department of Surgical Sciences, Radiology, Uppsala University, Uppsala, Sweden

7 Department of Neuroradiology, University Hospital Freiburg, Germany

2

Corresponding author

Tianyi Qian,

tianyiresearch@163.com

Siemens Healthcare China, MR Collaboration

7# Wangjing Zhonghuan Nanlu, Beijing, China

Phone: +86 18612442638   Fax:+86-10-64764951

Running head

Iterative Approach of RS-fMRI Perfusion

Key words

Resting-state functional connectivity magnetic resonance imaging (R-fMRI), Default mode network, Cerebral vascular territories, Time-shift mapping, Iterative algorithm

3

ABSTRACT

Introduction

RS-fMRI is based on the assumption that the vascular response and the blood oxygenation level dependent (BOLD) response are homogenous across the entire brain. However, this a priori hypothesis is not consistent with the well-known variability of cerebral vascular territories. In order to explore whether the RS networks are influenced by varied vascular speed in different vascular territories, we assessed the time-shift maps that give an estimate of the local timing of the vascular response and check whether local differences in this timing have an impact on the estimates of RS networks.

Methods

217 elderly (>=60 years), healthy participants (73.74 ± 4.41 years, 143 female, 203 right-handed) underwent one MRI examination including an RS-fMRI session. After preprocessing, statistical analyses included time-shift analyses and RS-fMRI analyses using as regressor the delay maps obtained from the time-shift analyses. The functional connectivity map of default mode network of each participant was then calculated by using the seed-to-voxel analysis in the REST toolbox.

Results

Faster cerebrovascular responses were notably present in the primary motor and somatosensory and peri-insular cortex while slower responses were present in various regions including notably the posterior cingulate cortex (PCC). Moreover, significant changes notably in the default mode network (DMN), including medial pre-frontal cortex (t=11.95), posterior cingulate cortex (t=11.52), right middle temporal lobe (t=10.72) and right angular gyrus (t=10.88), were observed also taking into account the cerebrovascular delayed maps.

4

Discussion

As the most prominent example of the RS networks, DMN activation patterns change as a function of the cerebrovascular delay. These data suggest that a group correction for vascular maps in RS-fMRI measurements is essential to correctly depict functional differences and exclude potential confounding effects, notably in the elderly with increasing prevalence of vascular co-morbidity.

5

INTRODUCTION

Resting state fMRI (RS-fMRI) measures the synchronized spontaneous low-frequency fluctuations of the BOLD signal in a task-free environment. The synchronizations are known to represent the functional connections of different brain areas (Fox and Raichle, 2007). RS-fMRI has been improving for the last 20 years and its applications extend from research to clinics (Barkhof *et al.*, 2014; Fox and Greicius, 2010)*.* The spotlight here is on the intrinsic brain activity in the absence of any sensory or cognitive stimulus (Smitha *et al.*, 2017). Application of this technique has allowed the identification of various Resting State Networks (RSNs) (Lee *et al.*, 2013). Among them, the Default Mode Network (DMN) has been exhaustively studied, and changes in the patterns of its activation have been repeatedly reported in a broad spectrum of neuropsychiatric disorders (Greicius, 2008; Laird *et al.*, 2011; Zhang and Raichle, 2010).

RS-fMRI assumes that the vascular response and the BOLD response are homogenous across the entire brain (Katanoda *et al.*, 2002; Yuan *et al.*, 2013). However, several ASL studies demonstrated that the patterns of vascular response vary substantially in neocortical areas (Emmert *et al.*, 2016; Hartkamp *et al.*, 2013; Wang *et al.*, 2014) as arterial spin labeling (ASL) MRI provides concomitant information on cerebral perfusion and brain anatomy allows for differentiating vascular territories in the brain (Damasio, 1983; Floyd *et al.*, 2003; Tatu *et al.*, 1998; 2012).. Although some previous studies suggested that the "back ground noise" from white matter, grey matter and CSF should be regressed out during the post-processing pipeline of RS-fMRI data (Murphy *et al.*, 2009; Schölvinck *et al.*, 2010; Shmueli *et al.*, 2007), the effects of vascular territories haven't been fully considered. It is thus possible that the functional connectivity of RS networks (and in particular the DMN) may change according to the differences in vascular speed.

6

In the present study, we assess the time-shift maps that give an estimate of the local timing of the vascular response using an innovative approach and examine whether local differences in the speed of the vascular response influence the functional connectivity of the DMN.

METHODS

Participants

217 elderly (>=60 years), community-dwelling healthy participants (mean age: 73.74 ± 4.41 years, 143 female, 203 right-handed) were enrolled in this study (Geneva and Lausanne). These community-based cases were recruited via advertisements in local newspapers and media. All participants had normal or corrected-to-normal visual acuity. Past hearing problems were identified as a part of the medical interview (including both subjects and their proxies). All cases with such problems were *a priori* excluded. All individuals were evaluated with an extensive neuropsychological battery, including the Mini-Mental State Examination (MMSE), the Hospital Anxiety and Depression Scale, and the Lawton Instrumental Activities of Daily Living (Haller et, al., 2017).

All individuals were also evaluated with the Clinical Dementia Rating scale. Only cases with intact cognitive abilities and CDR score of 0 were included in our sample. The education level was defined according to the Swiss scholar system, where level 1 = less than 9 years (primary school), level 2 = between 9 and 12 years (high school), and level 3 = more than 12 years (university).

This study was approved by the Commission cantonale d'éthique de la recherche Genève (cantonal ethics committee Geneva) and has been performed in accordance with the ethical standards prescribed in the 1964 Declaration of Helsinki and its later amendments. Written consent was obtained from all participants in accordance with the local guidelines.

7

MRI data acquisition

MRI exam included routine protocols for screening obvious lesions and a resting-state fMRI (rs-fMRI) session. The rs-fMRI data acquisition used an echo-planar imaging (EPI) sequence with the parameters as follows: TR=2000 ms, TE=30 ms, flip angle=90°, 33 slices, slice thickness=3.5 mm, distance factor=20%, FOV=210 ×210 mm^2, matrix= 64×64, measurements=200. A high-resolution T1-weighted magnetization prepared rapid gradient echo (MPRAGE) dataset (TR =2300ms, TE=2.27ms, 176 slices, 1mm isotropic, FOV= 256 × 256 mm^2, matrix= 256×256) was acquired as anatomical reference. All data were collected on a MAGNETOM Trio Tim 3T MR scanner (Siemens Healthcare, Erlangen, Germany) using a 32-channel head-coil.

Pre-processing of fMRI data

The fMRI data was firstly pre-processed with a standard pipeline for resting-state data analysis by using GRENTA toolbox (https://www.nitrc.org/projects/gretna) in MATLAB. The pipeline included slice timing correction, rigid head motion correction, normalization from individual space to standard MNI space by using EPI templates and re-sampling to 3mm isotropic, smoothing (FWHM=6 mm), de-trend and band-pass filter data with residual signals within 0.1-0.01Hz to remove the low-frequency signal drift.

Time-shift analysis

After the pre-processing, the time-shift map of each participant was calculated using an iterative algorithm with the following steps: 1) Averaging the time series of the whole brain to create the first time series template (time points from 6TR to 194TR). 2) For each voxel, the time course was shifted from -6TR to +6TR and correlated with the time series template at each TR. Each voxel was then labeled as the number of TR which had the maximum correlation coefficient value, and this value (ranged from -6 to +6) was defined as time-shift value of the voxel. 3) Shifting the time series of all voxels based on their relative time-shift value determined by step2. For example, if the -2TR has the largest

8

correlation coefficient with the template, then the time point at -2TR was set to time point 0, the rest of the time series were shifted with the same number of TRs in the timeline. 4) Averaging the re-aligned time series of the whole brain to create a new global time series template. 5) Repeating steps 2,3 and 4 until the number of voxels, that had changed their time-shift value between two iterations, is less than 100. 6) Smoothing the final time-shift value of all voxels using Gaussian kernel (FWHM =6 mm). 7) Subtracting the time-shift value of each voxel by the mean value of all voxel. The result of this step was defined as time-shift map (TSM).

The TSM of all participants were then averaged to create a TSM of the elder group. The distributions of time-shift values in different vascular territories were analyzed according to a custom-made atlas (based on previous knowledge of vascular territories and watershed areas WSA as depicted in Radiopaedia.org, courtesy of Dr Frank Gaillard and the IMAIOS online atlas https://www.imaios.com/en/e-Anatomy/Head-and-Neck/Brain-MRI-3D).

The time-shift map of each participant was then converted to z-score for group analysis. Voxel-based analysis of the normalized time-shift map in group level was performed by using two-sample t-test in the Resting-State fMRI Data Analysis Toolkit (REST), version 1.8 (Song *et al.*, 2011) to test the age effect to TSM. The differences between the younger group (<70 years, 70-) and elder group (>80 years, 80+) was investigated with gender and education as covariates. The clusters in the t-maps of group analysis were selected under a combined threshold of p<0.001 and a cluster size of 351 mm[3]. This yielded a corrected threshold of p < 0.05, determined by Monte Carlo simulation using the AlphaSim program with parameters: FWHM = 6 mm, within the brain mask (afni.nimh.nih.gov/pub/dist/doc/manual/AlphaSim.pdf). The variance of the time-shift value of each voxel among all participants was also calculated to test which areas had large individual differences.

9

Functional connectivity analysis

After the pre-processing steps of fMRI data, the residual signal in the frequency band of 0.1-0.01Hz was further processed by regressing out the background noise with two different methods. The first method used the regressor created by averaging the time-series of all voxels directly. The second method applied the global time-series template obtained in the TSM analysis as regressor and shifted the regressor according to the time-shift value for each voxel using an in-house developed MATLAB code. The functional connectivity map of the DMN of each participant was then calculated by using the seed-to voxel analysis in REST toolbox. The seed was located in posterior cingulate cortex (PCC, MNI coordinate: X=1 Y=-61 Z=38) with 6 mm radius, and the voxels with correlation coefficient value smaller than 0.2 were masked as 0. Fisher's Z-transform and paired t-test were used to compute the differences in functional connectivity between the datasets processed by two different noise regress strategies.

RESULTS

The averaged time-shift map of the rs-fMRI data over 217 normal participants is shown in Figure 1. The blue-purple represents negative time-shift meaning that blood flow arrives in this area earlier than the averaged time-shift value among all voxels of the brain, while yellow-red represent positive time-shift value and late arrival time. The motor, somatosensory and peri-insular cortex have the shortest while the frontal, parietal and temporal lobes including regions of the DMN notably the posterior cingulate cortex (PCC) and lateral ventricle shows the longest time-shift values.

A vascular territories mask was applied to assess the distribution of the time-shift value in different vascular territories. The box plot in Figure 2 illustrates that the MCA territory has the earliest blood arrival time (median value = 140ms, 25th percentiles= 67ms and 75th percentiles= 211ms) followed by the ACA (median value = 56ms, 25th percentiles= -35ms and 75th percentiles= 152ms) and finally PCA territories (median value = 8ms, 25th percentiles= -108ms and 75th percentiles= 99ms).

10

Figure 3 and Table 1 show the group differences between 70- and 80+. As compared to the 70- group, the 80+ group has longer time-shift in the frontal horn of the lateral ventricle and the body of the lateral ventricle, with shorter time-shift values in left parahippocampal gyrus.

As shown in Figure 4, the time-shift values have large variance in ventricles, brain stem, temporal lobe, and inferior frontal lobes. When comparing the variance in different vascular territories (figure 5), the PCA (median value = 0.81, 25th percentiles= 0.66 and 75th percentiles= 1.05) territory displays a more pronounced variance compared to ACA (median value = 0.69, 25th percentiles= 0.54 and 75th percentiles= 0.79) and MCA (median value = 0.66, 25th percentiles= 0.54 and 75th percentiles= 0.79).

In respect to the functional connectivity maps of DMN in a single participant (figure 6), an enhanced correlation coefficient between the seed (in PCC) and the medial prefrontal cortex (mPFC) could be observed in maps obtained from the data processed by the time-shift regression method compared to the global average regression. The results of the paired t-test between the two co-variance regression strategies shown in figure 7 indicate that the time-shift regression method could enhance the connectivity within the DMN including PCC, medial pre-frontal cortex (mPFC), middle temporal lobe, and angular gyrus.

DISCUSSION

To our knowledge, this is the first study that evaluates the impact of the local timing of the vascular response on RS network functional connectivity patterns. Using innovative time-shift maps, our results show first that vascular speeds vary across the different cortical areas in the absence of external stimuli. Secondly, we demonstrate that take into account the 'reactivity maps' previously extracted, changes in RS-fMRI network activation in terms of delayed responses are present mainly in the periphery of the DMN.

11

The present findings show regional differences in terms of vascular speed notably in the pre-central gyrus and motor cortex. These regions have therefore different timing of blood flow arrival than the rest of the brain. These results are in line with previous observations using breath-holding, showing changes in vascular reactivity between different parts of the brain (Geranmayeh *et al.*, 2015; Iranmahboob *et al.*, 2016; Lipp *et al.*, 2015; Tancredi and Hoge, 2013). The motor cortex and pre-central gyrus include representations of the respiratory muscles (Colebatch *et al.*, 1991; Li and Rymer, 2011). This can partly explain the differences in cerebrovascular response of these brain areas.

After creating the 'delayed maps' from the vascular response, we proceeded to take these maps into the RS analyses, using the DMN as the most prominent example. Our findings reveal significant differences in RS DMN functional connectivity patterns (in particular in its periphery) when taking into account the 'delayed maps' of vascular response. In particular, the time-shift regression method could enhance the connectivity within the DMN including PCC, medial pre-frontal cortex (mPFC), middle temporal lobe, and angular gyrus. These results are in line with previous works investigating changes in the cerebrovascular reactivity (Golestani *et al.*, 2016; Haight *et al.*, 2015), showing that the BOLD signal is potentially mediated by concomitant alterations in the cerebrovascular response. Our observations support the idea that the presence of varied in cerebro-vascular response may be the major vascular modulator of RS-fMRI (Golestani *et al.*, 2016). The present results imply that not taking into account any vascular information is a good approximation, yet it is not totally accurate. In line with previous studies (Golestani *et al.*, 2016), we suggest a group correction for vascular maps in RS-fMRI analyses, to depict cerebrovascular differences and exclude potential confounding effects.

Functional connectivity analyses, regardless whether seed-based or ICA-based, intrinsically assume that the vascular BOLD response to neuronal activation is equal across the brain. We however know from vascular anatomy, that this is not the case. The known vascular variations in the blood supply of the brain have been ignored in most fMRI studies, yet may cause a systematic and local effect in the brain - while other physiological parameters such as e.g respiration in general affects the entire brain globally. Without the cerebro-vascular response, the BOLD signal after standard pre-processing steps may still contain

12

the perfusion related pattern, but in different phases across different brain areas. This type of "noise" will reduce the correlation coefficient when running functional connectivity analysis. By regressing out the global averaged signal, this perfusion pattern could be removed from the areas that are in the same phase of the global pattern, but still exist in the voxels containing perfusion patternss in different phases.

DMN is a widely distributed network that has areas located in at least two brain-vascular territories, ACA and MCA. It is further know that the DMN recovers in an anterio-posterior temporal gradient when switching from task to rest (Van et, al., 2012).

The correlation coefficient value between PCC and mPFC will be affected by the brain-vascular response time in ACA and MCA. The shifted regressor can provide better modeling of the BOLD fluctuation due to brain-vascular response.remove this part of noise can further improve the accuracy of real functional connectivity without "perfusion relationship". Several brain-vascular territories based regressors' combination could also been considered to remove this component, paralleling the idea of modeling of the physiological patterns proposed in a previous study (Catie Chang, et al., 2009). Our results could further demonstrate that when taking into account this local variationss in time shift, this may indeed and as expected increase the estimated correlation.

Besides their neuroradiological relevance, our observations may also have clinical significance. Small but notable differences in the cerebro-vascular response may be particularly important in a clinical population. In fact, elderly individuals (80+) may have stronger variation in cerebrovascular response as compared to younger controls (70-) due to increasing prevalence of vascular co-morbidity. The observed variations of this parameter between cases younger than 70 years and older than 80 years of age further suggest that this hemodynamic parameter may display significant fluctuations in elderly individuals due to vascular morbidities. Consequently, vascular-related confounding effects on RS-fMRI may be stronger in very old individuals. Therefore, when performing RS analyses in young volunteers, correcting for vascular maps might not generate prominent differences. However, in an older cohort with vascular comorbidity the situation may be very different.

13

The temporal delay in BOLD signals has first been investigated in acute stroke by Yating et, al., (Lv *et al.*, 2013). Some other groups also tried to calculate the time delay of the lesion area in ischemic stroke and Moyamoya patients (Christen *et al.*, 2015; Khalil *et al.*, 2017; Siegel *et al.*, 2016). These studies used the averaged time-series of BOLD signal within a whole-brain mask or manually picked ROI as the template of fluctuation pattern to measure the time delay. Due to the changed time-shift in different vascular territories, simply averaging the time-series of all voxels together will mix the patterns in different phases. The manually selected ROI might have subjective bias and might also lead to unclear patterns due to the insufficient SNR. One of our previous study (Qian et al., 2015) showed that the abnormal perfusion areas detected with iterative algorithms were more consistent with dynamic susceptibility contrast MR than the method without iteration. In such cases, the iterative algorithm proposed in this study could extract the time series pattern automatically and more accurately. Although the results in normal subjects were closely match to the known anatomic vascular territories, this algorithm still based on the hypothesis that the first template obtained by average the time-series of all brain voxels still keeps the main pattern for calculating time-shift map. However, this hypothesis may not always correct, (e.g. using the prior knowledge of whole brain perfusion pattern may improve the starting template in the iterative algorithm). In this study, we didn't acquire any CT/MR perfusion data with contrast agent injected. So the accuracy and reliability of this method in normal subjects still need to be evaluated in future study.

To conclude, the present study aims to specifically assess the time-shift maps that give an estimate of the local timing of the vascular response and to check whether local differences in the speed of the vascular response influence the estimated RS networks. Our results show that taking into account the cerebrovascular delayed maps slightly modify the DMN as the most prominent example of the RSNs. Therefore, we suggest that a group correction for vascular maps in RS-fMRI measurements is essential to correctly depict functional differences and to exclude potential confounding effects.

14

LIMITATIONS

Two main limitations should be considered when interpreting our data. First, the present analysis is confined to the DMN and does not address the impact of the cerebro-vascular reactivity on other RSNs activation patterns. Second, the temporal resolution of the BOLD signal was only 2000ms, so we can only detect the large time-delay. Future works should extend this investigation and study possible influences of cerebro-vascular reactivity on other RSNs. Moreover, a simultaneous-multi-slice EPI sequence to acquire BOLD signal in higher spatial and temporal resolution should be applied to detect the time-delay more accurately.

Acknowledgements

The authors would like to acknowledge Dr. Ignacio Vallines, Dr. Aurelien Stalder, & Dr. Yi Sun for discussing this research project and giving useful suggestions during the preparation of the manuscript.

Disclosure

Tianyi Qian is an employee of Siemens Healthcare.

REFERENCES

Barkhof F, Haller S, Rombouts SARB. Resting-state functional MR imaging: a new window to the brain. Radiology 2014; 272: 29–49.

Christen T, Jahanian H, Ni WW, Qiu D, Moseley ME, Zaharchuk G. Noncontrast mapping of arterial delay and functional connectivity using resting-state functional MRI: a study in Moyamoya patients. J Magn Reson Imaging 2015; 41: 424–430.

Colebatch JG, Adams L, Murphy K, Martin AJ, Lammertsma AA, Tochon-Danguy HJ, et al. Regional cerebral blood flow during volitional breathing in man. J. Physiol. (Lond.) 1991; 443: 91–103.

Damasio H. A computed tomographic guide to the identification of cerebral vascular territories. Arch. Neurol. 1983; 40: 138–142.

Emmert K, Zöller D, Preti MG, Van De Ville D, Giannakopoulos P, Haller S. Influence of Vascular Variant of the Posterior Cerebral Artery (PCA) on Cerebral Blood Flow, Vascular Response to CO2 and Static Functional Connectivity. PLoS ONE 2016; 11: e0161121.

Floyd TF, Ratcliffe SJ, Wang J, Resch B, Detre JA. Precision of the CASL-perfusion MRI technique for the measurement of cerebral blood flow in whole brain and vascular territories. J Magn Reson Imaging 2003; 18: 649–655.

Fox MD, Greicius M. Clinical applications of resting state functional connectivity. Front Syst Neurosci 2010; 4: 19.

Fox MD, Raichle ME. Spontaneous fluctuations in brain activity observed with functional magnetic resonance imaging. Nat. Rev. Neurosci. 2007; 8: 700–711.

Geranmayeh F, Wise RJS, Leech R, Murphy K. Measuring vascular reactivity with breath-holds after stroke: a method to aid interpretation of group-level BOLD signal changes in longitudinal fMRI studies. Hum Brain Mapp 2015; 36: 1755–1771.

16

Golestani AM, Kwinta JB, Strother SC, Khatamian YB, Chen JJ. The association between cerebrovascular reactivity and resting-state fMRI functional connectivity in healthy adults: The influence of basal carbon dioxide. Neuroimage 2016; 132: 301–313.

Greicius M. Resting-state functional connectivity in neuropsychiatric disorders. Current Opinion in Neurology 2008; 21: 424–430.

Haight TJ, Bryan RN, Erus G, Davatzikos C, Jacobs DR, D'Esposito M, et al. Vascular risk factors, cerebrovascular reactivity, and the default-mode brain network. Neuroimage 2015; 115: 7–16.

Hartkamp NS, Petersen ET, De Vis JB, Bokkers RPH, Hendrikse J. Mapping of cerebral perfusion territories using territorial arterial spin labeling: techniques and clinical application. NMR Biomed 2013; 26: 901–912.

Iranmahboob A, Peck KK, Brennan NP, Karimi S, Fisicaro R, Hou B, et al. Vascular Reactivity Maps in Patients with Gliomas Using Breath-Holding BOLD fMRI. J Neuroimaging 2016; 26: 232–239.

Katanoda K, Matsuda Y, Sugishita M. A spatio-temporal regression model for the analysis of functional MRI data. Neuroimage 2002; 17: 1415–1428.

Khalil AA, Ostwaldt A-C, Nierhaus T, Ganeshan R, Audebert HJ, Villringer K, et al. Relationship Between Changes in the Temporal Dynamics of the Blood-Oxygen-Level-Dependent Signal and Hypoperfusion in Acute Ischemic Stroke. Stroke 2017; 48: 925–931.

Laird AR, Fox PM, Eickhoff SB, Turner JA, Ray KL, McKay DR, et al. Behavioral interpretations of intrinsic connectivity networks. J Cogn Neurosci 2011; 23: 4022–4037.

Lee MH, Smyser CD, Shimony JS. Resting-state fMRI: a review of methods and clinical applications. AJNR Am J Neuroradiol 2013; 34: 1866–1872.

Li S, Rymer WZ. Voluntary breathing influences corticospinal excitability of nonrespiratory finger muscles. J. Neurophysiol. 2011; 105: 512–521.

17

Lipp I, Murphy K, Caseras X, Wise RG. Agreement and repeatability of vascular reactivity estimates based on a breath-hold task and a resting state scan. Neuroimage 2015; 113: 387–396.

Lv Y, Margulies DS, Cameron Craddock R, Long X, Winter B, Gierhake D, et al. Identifying the perfusion deficit in acute stroke with resting-state functional magnetic resonance imaging. Ann Neurol. 2013; 73: 136–140.

Murphy K, Birn RM, Handwerker DA, Jones TB, Bandettini PA. The impact of global signal regression on resting state correlations: are anti-correlated networks introduced? Neuroimage 2009; 44: 893–905.

Schölvinck ML, Maier A, Ye FQ, Duyn JH, Leopold DA. Neural basis of global resting-state fMRI activity. Proceedings of the National Academy of Sciences 2010; 107: 10238–10243.

Shmueli K, van Gelderen P, de Zwart JA, Horovitz SG, Fukunaga M, Jansma JM, et al. Low-frequency fluctuations in the cardiac rate as a source of variance in the resting-state fMRI BOLD signal. Neuroimage 2007; 38: 306–320.

Siegel JS, Snyder AZ, Ramsey L, Shulman GL, Corbetta M. The effects of hemodynamic lag on functional connectivity and behavior after stroke. J. Cereb. Blood Flow Metab. 2016; 36: 2162–2176.

Smitha KA, Akhil Raja K, Arun KM, Rajesh PG, Thomas B, Kapilamoorthy TR, et al. Resting state fMRI: A review on methods in resting state connectivity analysis and resting state networks. Neuroradiol J 2017; 30: 305–317.

Song X-W, Dong Z-Y, Long X-Y, Li S-F, Zuo X-N, Zhu C-Z, et al. REST: a toolkit for resting-state functional magnetic resonance imaging data processing. PLoS ONE 2011; 6: e25031.

Tancredi FB, Hoge RD. Comparison of cerebral vascular reactivity measures obtained using breath-holding and CO_2 inhalation. J. Cereb. Blood Flow Metab. 2013; 33: 1066–1074.

Tatu L, Moulin T, Bogousslavsky J, Duvernoy H. Arterial territories of the human brain: cerebral hemispheres. Neurology 1998; 50: 1699–1708.

18

Tatu L, Moulin T, Vuillier F, Bogousslavsky J. Arterial territories of the human brain. Front Neurol Neurosci 2012; 30: 99–110.

Wang R, Yu S, Alger JR, Zuo Z, Chen J, Wang R, et al. Multi-delay arterial spin labeling perfusion MRI in moyamoya disease--comparison with CT perfusion imaging. Eur Radiol 2014; 24: 1135–1144.

Yuan R, Di X, Kim EH, Barik S, Rypma B, Biswal BB. Regional homogeneity of resting-state fMRI contributes to both neurovascular and task activation variations. Magn Reson Imaging 2013; 31: 1492–1500.

Zhang D, Raichle ME. Disease and the brain's dark energy. Nat Rev Neurol 2010; 6: 15–28.

Qian T, Wang Z, Gao P. Measuring the timing information of blood flow in acute stroke with the "background noise" of BOLD Signal. ISMRM2015, Toronto.

Chang C, Cunningham J, Glover G. Influence of heart rate on the BOLD signal: The cardiac response function. NeuroImage 2009; 44: 857-869

Haller S, Montandon ML, Rodriguez C, Ackermann FR, Herrmann FR, Giannakopoulos P. APOE*E4 Is Associated with Gray Matter Loss in the Posterior Cingulate Cortex in Healthy Elderly Controls Subsequently Developing Subtle Cognitive Decline. Am J Neuroradiol 2017; 38(7):1335-1342.

Van De Ville D, Jhooti P, Haas T et al. Recovery of the default mode network after demanding neurofeedback training occurs in spatio-temporally segregated subnetworks. Neuroimage 2012; 63(4):-1775-1781.

19

Acronyms

ACA: Anterior Cerebral Artery

ASL: Arterial Spin Labeling

BOLD: Blood Oxygenation Level Dependent

DMN: Default Mode Network

EPI: Echo-Planar Imaging

MCA: Middle Cerebral Artery

mPFC: Medial Pre-Frontal Cortex

PCC: Posterior Cingulate Cortex

RS-fMRI: Resting State Functional MRI

RSNs: Resting State Networks

TSM: Time-Shift Map

20

Table 1. Regions showing decreased and increased time-shift value identified by age effect.

Brain Regions	MNI coordinate			Cluster size	t score
	X	Y	Z		
70- < 80+					
	-24	-45	-12	16	3.54
70- > 80+					
	39	-45	0	25	-3.38
	12	24	9	15	-3.90
	30	-39	18	46	-3.51

21

Table 2. Regions showing increased functional connectivity with time-shift compared to global average regression.

Brain Regions	MNI coordinate			Cluster size	t score
	X	Y	Z		
Medial pre-frontal cortex	3	60	12	1402	11.95
Posterior cingulate cortex	-6	-45	42	756	11.52
Middle Temporal lobe (Right)	60	-15	-18	109	10.72
Angular gyrus (Right)	42	-57	36	107	10.88

FIGURE CAPTIONS
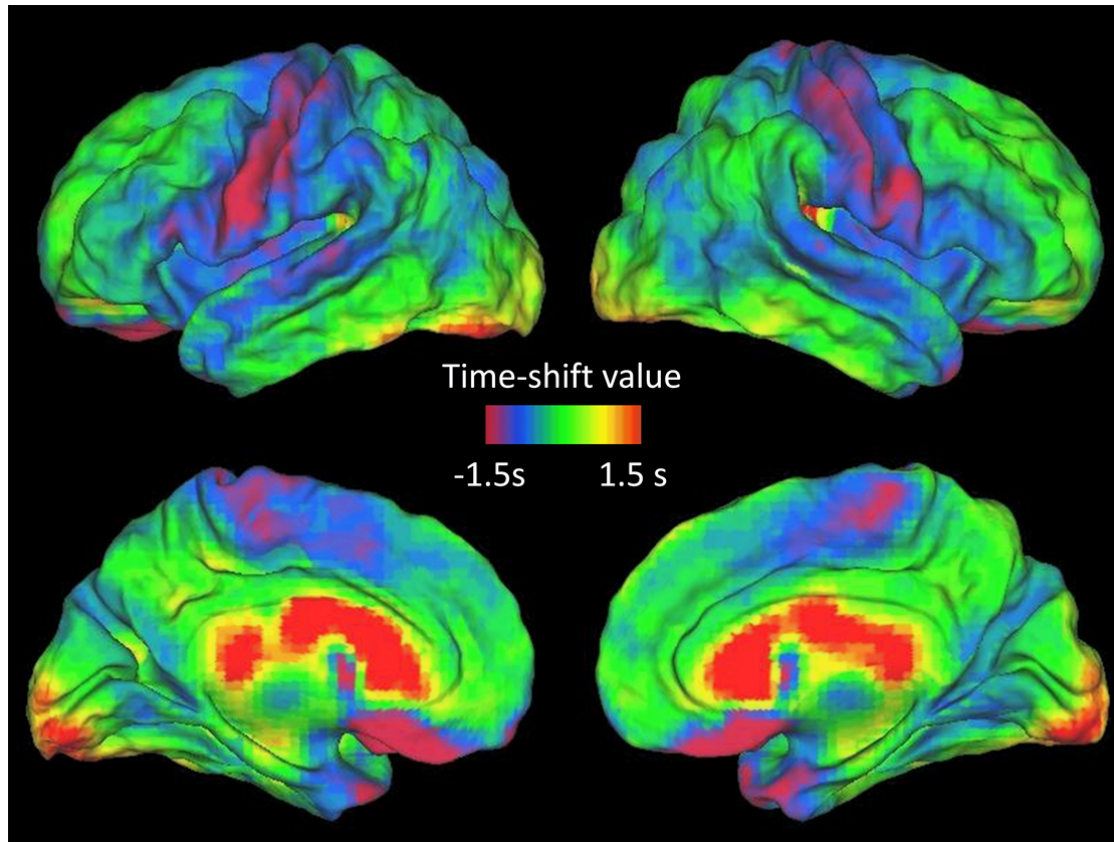
Figure 1, Averaged time-shift maps obtained from resting-state-fMRI data of 217 healthy participants. The blue-purple represents the blood flow that arrives in this area earlier than average while yellow-red represents a late arrival.

23
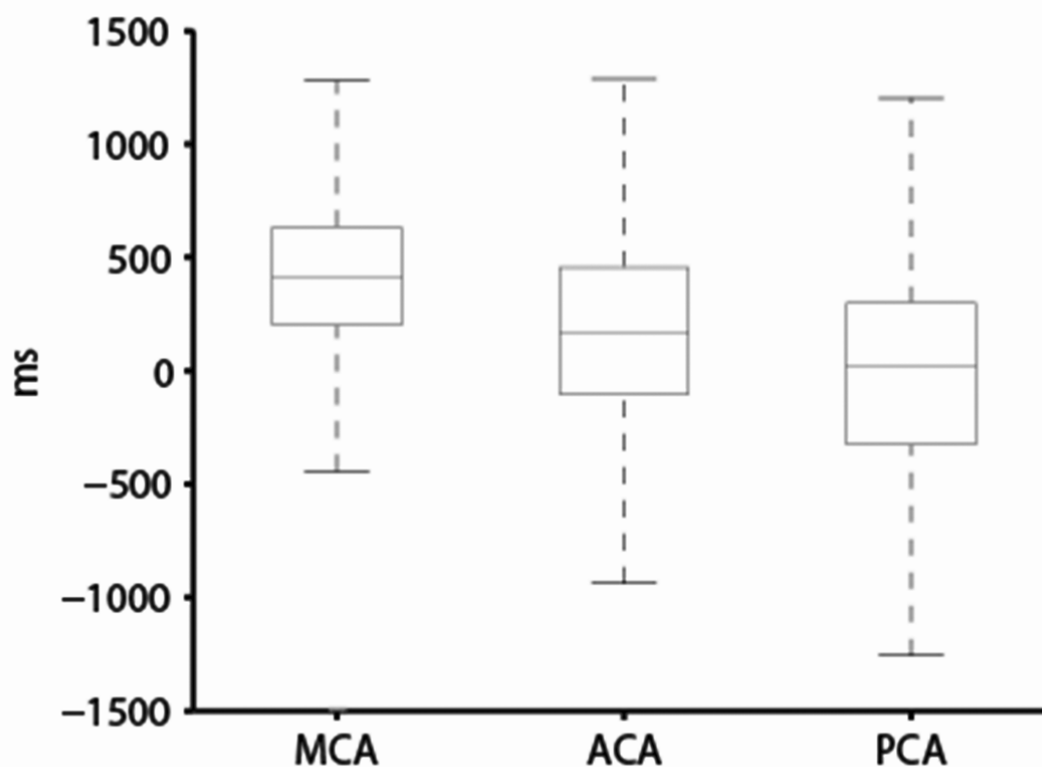
Figure 2, The statistic results of the time-shift value of voxels in different vascular territories. MCA: middle cerebral artery, ACA: anterior cerebral artery, PCA: posterior cerebral artery.
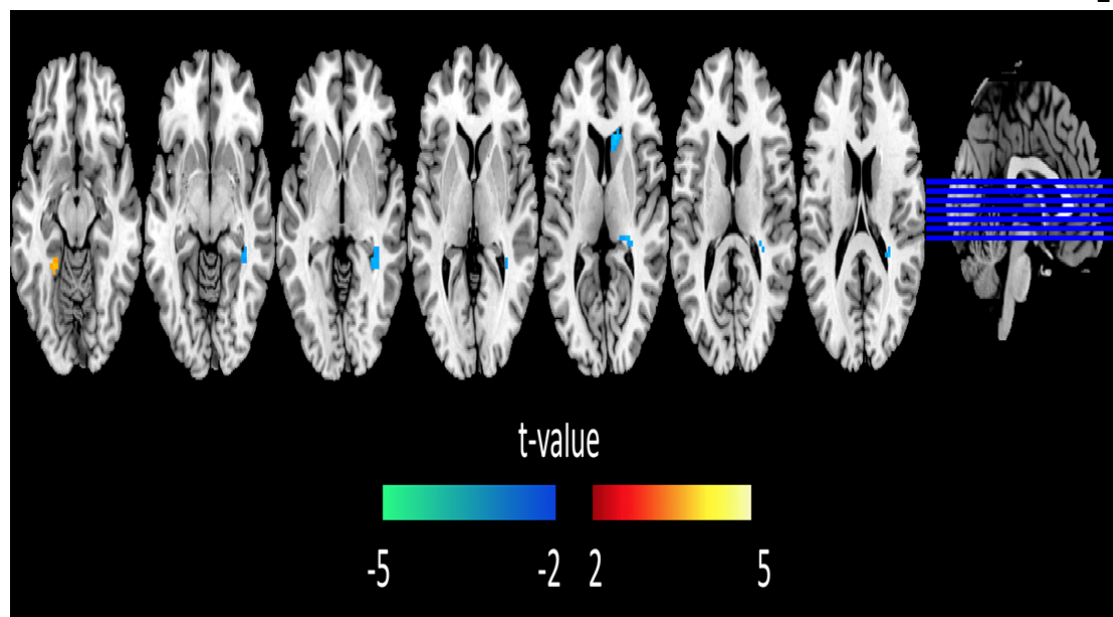
24

Figure 3, Group differences between 70- and 80+ cases, based on a 2-sample t-test with gender and education as covariates. The threshold was set to a corrected threshold of p <0.05, determined by AlphaSim (threshold = p<0.001). The color scale represents t-values. Green-Blue color represents longer time-shift in 80+ as compared to 70-.
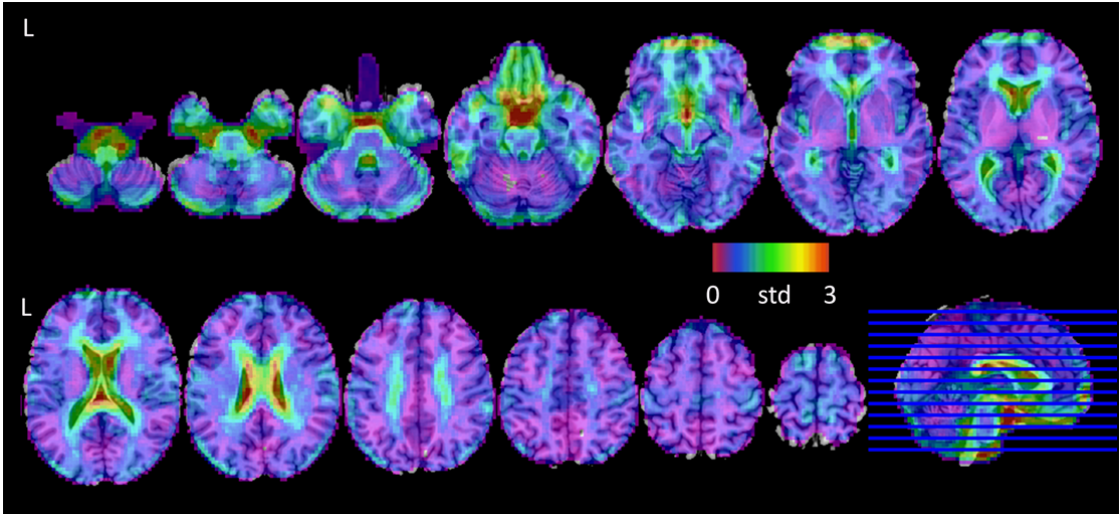
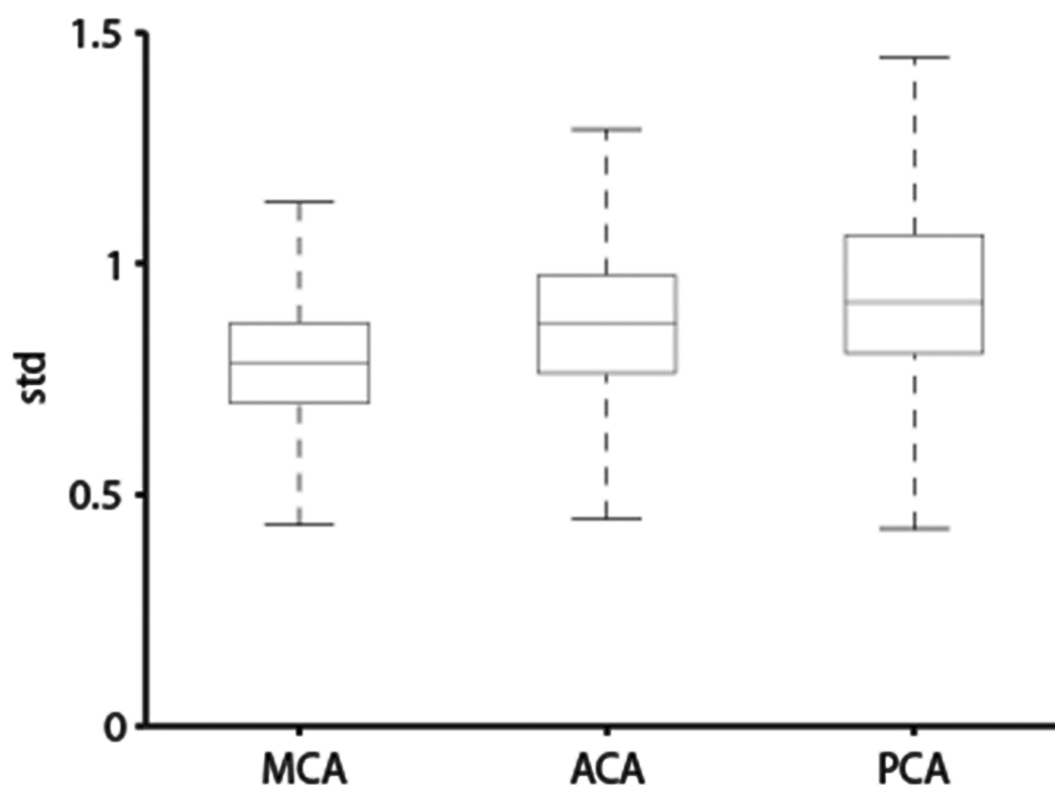Figure 4, Cross-participants variability of time-shift map.

Figure 5, Cross-participants variability of time-shift values in different vascular territories.

MCA: middle cerebral artery, ACA: anterior cerebral artery, PCA: posterior cerebral artery.
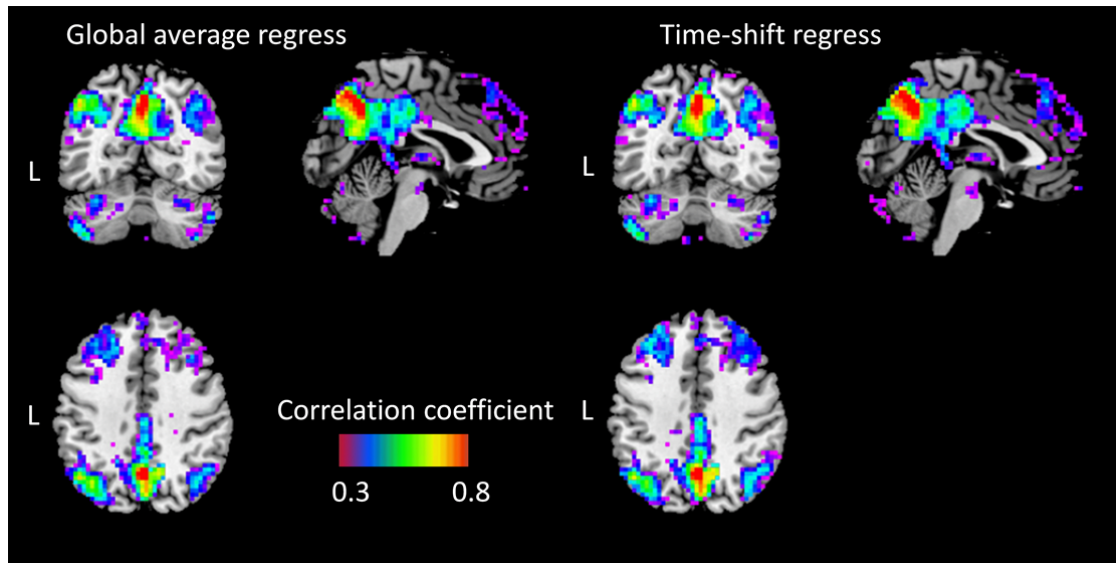
Figure 6, Functional connectivity map of the DMN obtained from two different types of co-variance regression strategies.
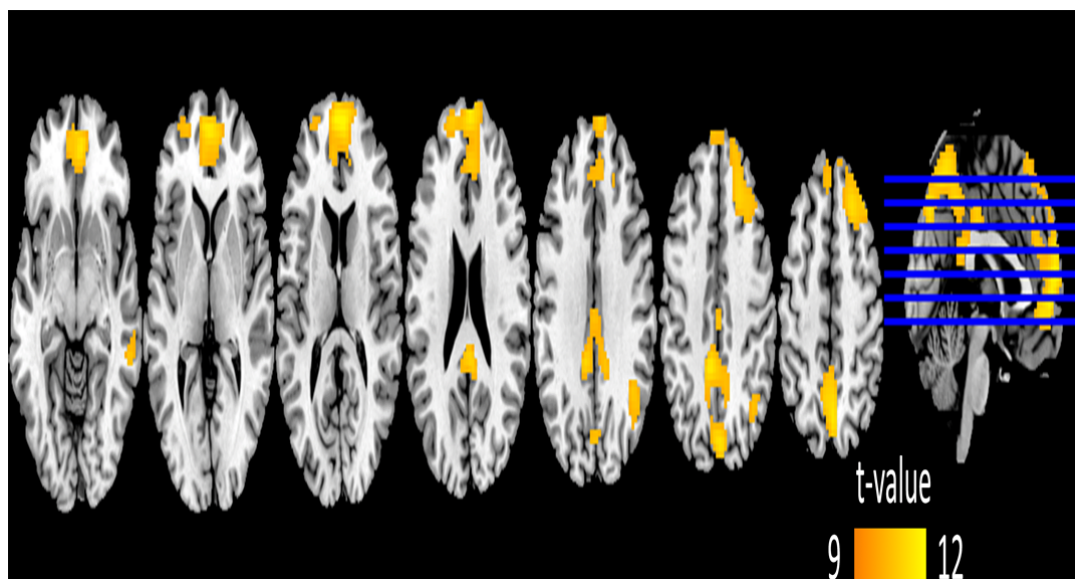
28

Figure 7, Time-shift regression versus global average regression differences of the functional connectivity maps among all participants. The orange-yellow represent higher correlation coefficient values with time-shift regression compared to global average regression.